

DOI: 10.1002/cphc.200800709

Chiral Gold Nanoparticles

Cyrille Gautier^[b] and Thomas Bürgi^{*[a]}

Monolayer-protected gold nanoparticles have many appealing physical and chemical properties such as quantum size effects, surface plasmon resonance, and catalytic activity. These hybrid organic–inorganic nanomaterials have promising potential applications as building blocks for nanotechnology, as catalysts, and as sensors. Recently, the chirality of these materials has attracted attention, and application to chiral technologies is an interesting perspective. This minireview deals with the preparation of chiral gold nanoparticles and their chiroptical properties. On the basis of the latter, together with predictions from quantum chemical

calculations, we discuss different models that were put forward in the past to rationalize the observed optical activity in metal-based electronic transitions. We furthermore critically discuss these models in view of recent results on the structure determination of some gold clusters as well as ligand-exchange experiments examined by circular dichroism spectroscopy. It is also demonstrated that vibrational circular dichroism can be used to determine the structure of a chiral adsorbate and the way it interacts with the metal. Finally, possible applications of these new chiral materials are discussed.

1. Introduction

Monolayer-protected gold nanoparticles (AuNPs) have attracted significant interest in recent years due to their importance in both fundamental science^[1–6] and technological applications such as catalysis,^[7,8] sensing,^[9,10] medicine, drug or DNA delivery,^[11] optics,^[12] photonics,^[13] and nanotechnology.^[14,15]

The physical properties of these organic–inorganic hybrid materials are highly tunable by changing not only the size and the shape of the gold core but also the spatial arrangement of these building blocks with respect to one another within a material.^[16,17] When the size of the AuNPs is reduced below the de Broglie wavelength of the conduction electrons (ca. 1 nm), the electronic structure observed in bulk gold or large AuNPs (>5 nm) evolves from quasicontinuous bands to discrete levels. Small AuNPs (<3 nm), also referred to as nanoclusters, are better described as semiconducting instead of metallic and no longer support the plasmon excitation characteristic of larger AuNPs.^[18] Preparation, properties, and potential applications of AuNPs have been extensively reviewed, but the notion of chirality has been put aside.^[14]

It is known that metal surfaces can exhibit intrinsically chiral structure.^[19] Furthermore, chirality can be bestowed onto achiral metal surfaces by adsorption of chiral molecules.^[20] Similarly, metal NPs can exhibit chirality, which is reflected by their optical activity in metal-based electronic transitions (MBETs). Transfer of chirality from the adsorbate to the metal surface depends on the structure of the former; however, this is difficult to elucidate. Due to their organic shell, monolayer-protected AuNPs can be dissolved in various solvents and are thus amenable to chiroptical techniques such as electronic circular dichroism (CD) and vibrational circular dichroism (VCD). The former has demonstrated its aptitude for the study of protein secondary and tertiary structures, whereas the latter has been used for the determination of conformation and absolute configuration of organic molecules in solution.^[21,22] Recently, these complementary techniques have been applied to AuNPs cov-

ered with different chiral organic ligands. Vibrational CD in the infrared region selectively probes molecular vibrations located in the organic shell, whereas CD in the UV/Vis region is sensitive to electronic transitions which may be located in the inorganic core. Here we demonstrate that VCD can be used to determine the structure of a chiral adsorbed molecule and the way in which it interacts with the metal. We review the preparation of chiral AuNPs and their chiroptical properties. On the basis of the latter, together with predictions from quantum chemical calculations, we discuss different models that were put forward in the past to rationalize the observed optical activity in MBETs. We furthermore critically discuss these models in view of recent results on the structure determination of some gold clusters as well as ligand-exchange experiments examined by CD spectroscopy. Finally, possible applications of these new chiral materials are discussed.

2. Preparation, Purification and Size Separation

2.1. Preparation

The literature dealing with metal NP synthesis is uncountable, and a wide variety of techniques have been reported using liquid-, solid-, and gas-phase precursors. Metal NPs can be prepared by the top-down (physical) approach. However, the

[a] Prof. Dr. T. Bürgi
University of Heidelberg
Physikalisch Chemisches Institut, Ruprecht-Karls-Universität
Im Neuenheimer Feld 253, 69120 Heidelberg (Germany)
Fax: (+49) 6221 54 49 18
E-mail: buergi@uni-heidelberg.de

[b] Dr. C. Gautier
Université de Neuchâtel, Institut de Microtechnique
Rue Emile-Argand 11, 2009 Neuchâtel (Switzerland)

bottom-up (chemical) approach is considerably cheaper and allows one to prepare very small particles.

The chemical approach is based on the nucleation and growth of metal atoms in liquid media or in the gas phase. The literature describes five general methods for chemical preparation of transition metal NPs: 1) Chemical reduction of metal salts, 2) ligand reduction and displacement from organometallic complexes, 3) electrochemical reduction, 4) metal vapor synthesis, and 5) thermal, photochemical, or sonochemical decomposition.

Among the huge number of methods listed in the literature, only a few have been used for the preparation of optically active metal NPs. A few examples of micro- and nanoparticle arrays (not necessarily of chiral NPs) with chiral shapes^[23] or chiral organizations^[24,25] have been studied theoretically^[24] or prepared by top-down methods such as electron-beam lithography and lift-off techniques.

Most optically active AuNPs have been prepared by the bottom-up approach, and more specifically by the chemical reduction of gold ions or of precursor complexes in solution.^[26] As shown in Figure 1, reduction of the gold salts is often per-

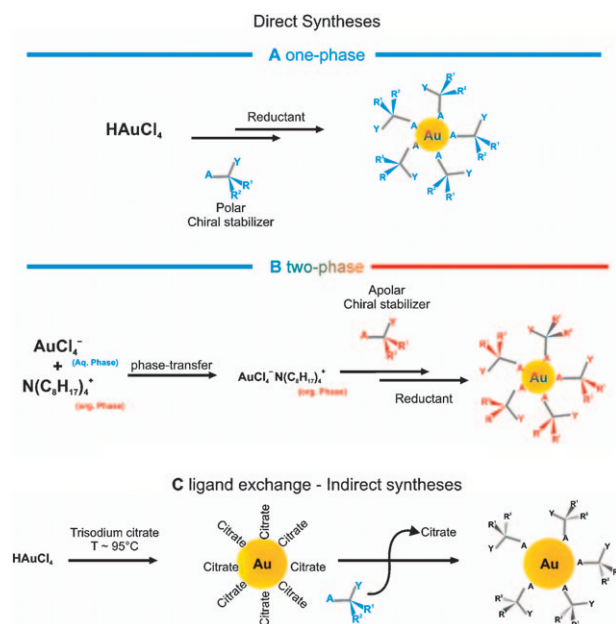


Figure 1. Different methods exploited for the syntheses of optically active AuNPs with chiral ligands.

formed in the presence of chiral stabilizers such as thiols, phosphines, and amines (DNA and alkaloids) in a one-pot procedure (direct syntheses). A) AuNPs are prepared in a single phase when the metal salt and the ligand are both soluble in the same solvent such as water, alcohols, acetic acid, tetrahydrofuran, or a mixture thereof. B) If their solubilities are not compatible, the Brust–Schiffrin synthesis^[27] provides ready access in a biphasic reaction taking advantage of phase-transfer compounds, generally tetraoctylammonium (TOA⁺) bromide, to shuttle ionic reagents to an organic phase where particle nucleation, growth, and passivation occur. C) When the

functional groups are not compatible with the reducing agent, the optical activity can be induced via post synthetic modification of the ligand shell, like a ligand-exchange reaction (indirect synthesis). This two-step method has some advantages in both purification and separation. Indeed, some AuNPs are very well characterized and both their separation and purification processes are well established.^[28] The AuNPs prepared by the citrate method of Turkevich et al.^[29] and those developed by Schmid,^[30] which are protected by triphenylphosphine, are surely the most frequently used AuNPs for the ligand exchange reaction. This strategy avoids the time-consuming search for efficient parameters for purification and separation of each new type of AuNPs. However, post-synthetic modifications such as ligand exchange in an excess of ligand often leads to a modification of the size distribution of the AuNPs.^[31–34]

2.2. Purification and Size Separation

The physical properties of NPs are strongly dependent on size and shape (Figure 2). For example, UV/Vis spectra of small AuNPs exhibit well-quantized and size-dependent electronic structure due to the quantum size effect (see Figure 2, right).

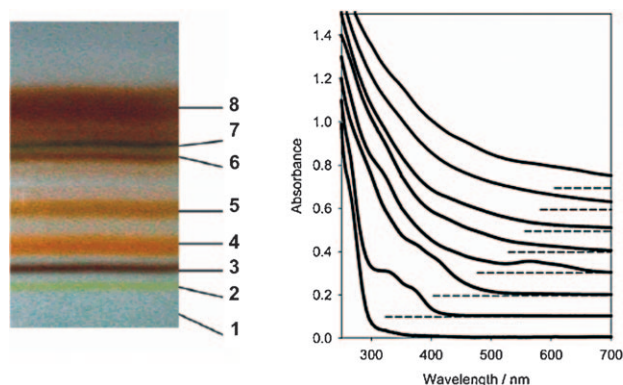


Figure 2. AuNPs separated according to their size by polyacrylamide gel electrophoresis (left). NPs are numbered according to increasing size. UV/Vis spectra of the size-separated AuNPs (right). A clear redshift of the absorption onset is observed as the size of NPs increases. Reprinted with permission from ref. [18]. Copyright (2006) American Chemical Society.

Fine tuning of properties for a specific purpose often requires perfect control of these two parameters, as well as a high degree of control of functionalization and purity. Procedures for the preparation of NPs are in constant progress, but till now only a few methods yield monodisperse particles with high purity.^[26,30,34–37] However, this fine-tuning can be performed after appropriate purification and separation processes. Current methods for purification of NPs samples, that is, removal of free ligand and reducing agent, involve centrifugation, precipitation, washing, dialysis, chromatography, or extraction to remove impurities. Size selection can be based on fractional crystallization, size exclusion chromatography (SEC), electrophoresis, and membrane-based methods such as ultrafiltration and diafiltration. These techniques are particularly appropriate for size separation of water-soluble NPs but are gen-

erally time-consuming and only viable for production on a small scale. The size separation of NPs soluble in organic media suffers from the lack of methods compatible with organic solvents. Fundamental studies on size-dependent chiroptical properties have been mainly performed with water-soluble NPs separated according to their size and charge by high-density polyacrylamide gel electrophoresis (PAGE; see Figure 2, left).^[118,38–41] Size selection of chiral NPs soluble in organic media has only been realized by SEC.^[42]

3. Vibrational Circular Dichroism: Conformational Study of Adsorbed Chiral Molecules

Vibrational circular dichroism (VCD) is the differential absorption of left and right circularly polarized infrared light;^[43] VCD spectra contain considerable structural information. The technique can be used to determine the absolute configuration of a sample without the need to grow single crystals. More importantly, it yields information on the conformation of dissolved molecules.^[44–47] This information must be extracted from the experimental spectrum by comparison with calculated spectra for the possible conformers. Generally the VCD spectra of different conformers differ significantly. Vibrational CD spectroscopy was recently applied for the first time to AuNPs of about 2 nm core diameter in order to study the conformation of adsorbed chiral cysteine derivatives.^[18,48–52] Figure 3 shows IR and VCD spectra of AuNPs covered by the

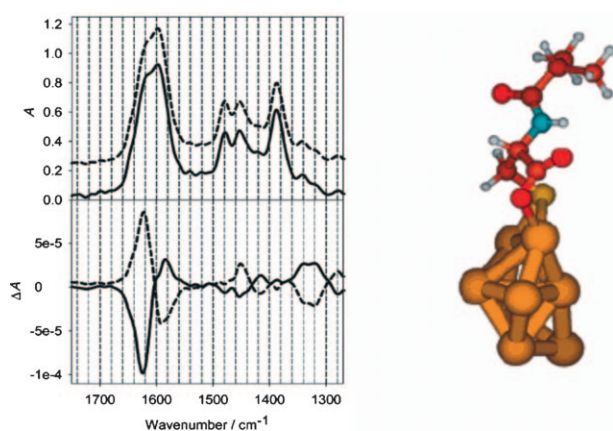


Figure 3. Infrared (top) and VCD (bottom) spectra of NIC-protected AuNPs. The dashed (solid) lines correspond to the spectra of the particles covered by the L enantiomer (D enantiomer). The calculated VCD spectrum of the conformer on the right on a Au₈ cluster best fits the experimental spectrum. Reproduced with permission from ref. [18]. Copyright (2006) American Chemical Society.

two enantiomers of *N*-isobutryl cysteine (NIC). Whereas the IR spectra are identical for the two enantiomers, the VCD spectra show a mirror-image relationship. Density functional theory (DFT) calculations show that the structure of the underlying gold cluster does not have a large effect on the simulated VCD spectra, whereas the conformation of the adsorbed thiol has a large influence. The calculated VCD spectrum of one stable conformer of NIC adsorbed on a small gold cluster matches

well with the experimental data. This conformation is characterized by an interaction of the carboxylate group with the gold cluster (see Figure 3). Thus, the carboxylate group seems to be a second anchoring point beside the strong Au–S bond. This two-point interaction may influence the optical activity of the NPs (see below).

4. Optical Activity in Metal-Based Electronic Transitions

It is tempting to assume that the structure of metal NPs corresponds to a fragment of the highly symmetric bulk crystal lattice. However, in 1996 calculations performed by Wetzel and DePristo and experimental observations by Riley et al. indicated that naked Ni₃₉ clusters prefer a lower symmetry (*D*₅) chiral structure.^[53,54] At the same time, Whetten and co-workers experimentally observed optical activity in the MBETs for a Au₂₈ cluster covered with L-glutathione (GSH), a chiral tripeptide.^[38] They furthermore isolated well-defined clusters of different mass by PAGE. The three smaller isolated clusters with a core mass between 4 and 8 kDa showed strong optical activity, whereas neither the crude mixture nor the higher molecular weight components have such strong optical activity. The optical activity in the near-infrared, visible, and near-ultraviolet is clearly size-dependent and can be attributed neither to the metal precursors nor to the organic species. Its amplitude is comparable to the signals observed for intrinsically chiral conjugated systems like chiral fullerenes or larger helicenes. However the key question remains whether the gold core is intrinsically chiral or not.

4.1. Possible Mechanism and Theoretical Studies

The observed optical activity in MBETs of small metal particles protected with chiral thiols can be attributed to two opposite and one intermediate models (see Figure 4). In the first, the optical activity arises from an intrinsically chiral inorganic core (A). In the presence of chiral ligands one of the two possible enantiomers of the core is favored. Such behavior is found for coordination clusters with a chiral framework.^[58–68] In the second, the inorganic core can be achiral and the optical activ-

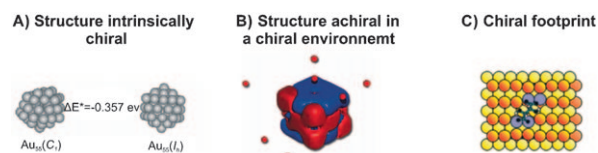


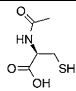
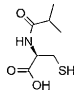
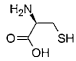
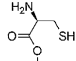
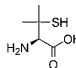
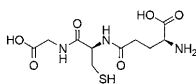
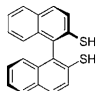
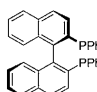
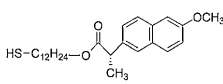
Figure 4. Possible origins of optical activity observed for metal particles. A) The calculated chiral structure (*C*₁) of bare Au₅₅ is more stable than the highly symmetric structure (*I*_h). Reprinted from ref. [55] with kind permission of The European Physical Journal (EPJ). B) Chiral distribution of electron density in Au₂₈ gold clusters induced by a chiral point-charge system. Red points correspond to negative point charges and red and blue surfaces in the core represent regions of high and low electron density, respectively. Reproduced from ref. [56] with permission of the PCCP Owner Societies. C) Chiral footprint imparted by bitartrate on Ni(100) surface. Reproduced with permission from ref. [57]. Copyright (2002) American Chemical Society.

ity is induced by a chiral environment (B) due to the chiral organic shell through a vicinal effect (B1: an achiral core with chiral ligands in achiral adsorption pattern) or through a chiral electrostatic field (B2: an achiral core with optical activity induced by a chiral adsorption pattern). Models A and B have support from theoretical calculations.^[55,56,69] Garzón et al. have predicted that small metal particles such as Au₂₈ or Au₅₅ prefer low-symmetry chiral over high-symmetry nonchiral structures.^[55,69] Goldsmith and co-workers demonstrated that optical activity could arise from an achiral metal core perturbed by a dissymmetric field originating from the chiral organic shell.^[56] In the intermediate model, the grand core can be achiral but the relaxation of the surface atoms involved in the adsorption of the chiral ligand creates a chiral "footprint", like that observed for adsorption of tartaric acid on Ni surfaces (C).^[57] This is favored for ligands that have at least two anchoring points on the surface. Such double interactions have indeed been documented on surfaces and seem to be a common characteristic of ligands that can induce intense optical activity in MBETs (vide infra).^[50,57,70–73] Density functional calculations have shown that the ligands not only play the role of passivating molecules, but they also distort the metal-cluster structure.^[55] In addition, Häkkinen and co-workers used DFT calculations to predict that the structure of an Au₃₈(SCH₃)₂₄ cluster consists of ringlike (AuSCH₃)₄ units protecting a central Au₁₄ core.^[74] It is likely that the three mechanisms concurrently impart optical activity to the core. The key question whether the core is chiral, whether only the surface of the core is chiral, or whether both the core and the surface are achiral remains unanswered at this point.

4.2. Circular Dichroism Studies

Recently, optical activity in MBETs has been reported for gold, silver, palladium, and CdS nanoclusters having a more or less well defined size and an organic shell composed of different chiral molecules.^[18,26,39,40,75–78] Table 1 shows the chemical structures of the different molecules that have been shown to induce optical activity in MBETs as well as the NP size and the

Table 1. Chemical structures of chiral molecules inducing optical activity on metal NPs.

Name	Structure	Metal/maximum anisotropy factor/size
<i>N</i> -acetyl-L-cysteine (NALC)		–
<i>N</i> -isobutyryl-L-cysteine (NILC)		Au/0.5 x 10 ⁻³ /1–2 nm
L-cysteine		–
L-cysteine methyl ester		Au/0/20–25 nm
L-penicillamine (L-pen)		Au/3 x 10 ⁻⁴ to 1 x 10 ⁻⁴ /0.57–1.75 nm and Au/1 x 10 ⁻³ to 1 x 10 ⁻⁵ /1–1.9 nm
L-glutathione		Au/2 x 10 ⁻⁴ to 1 x 10 ⁻³ /0.7–1 nm
(<i>R</i>)-BINAS		Au/4 x 10 ⁻³ /1–2 nm
(<i>R</i>)-BINAP		Au/4 x 10 ⁻³ /1–2 nm
(<i>S</i>)-naproxen-functionalized-alkanethiol (C ₁₂ Napr*9)		–

maximum of amplitude of the anisotropy factor (g_{\max} factor) measured for AuNPs or AgNPs.

4.2.1. General Observations

Pairs of metal clusters with similar inorganic core, size or size distribution, and the same number and type of ligands but with opposite absolute configuration exhibit mirror-image CD spectra like common chiral molecules do. No optical activity is observed for gold and silver clusters prepared with a racemic mixture of ligand.^[39,79] Interestingly, the UV/Vis spectra reported for each fraction of size-separated D-Pen-, L-Pen-, and *rac*-Pen-protected AuNPs (Pen = penicillamine) are identical, whereas in the case of silver particles, the UV/Vis spectra of the *rac*-Pen-protected particles are slightly different from the homochiral ones.^[39,79] These considerations indicate that the structure of the AgNPs is more dependent on the composition of the organic shell than in the case of AuNPs. It is thus tempting to speculate that mechanism C has a larger effect in the case of silver, maybe due to its lower cohesive energy.

4.2.2. Size Effect

In all cases where optical activity in size-selected NPs was observed, the CD signals change with the size of the NPs. In most cases the anisotropy factor gradually increases with decreasing mean cluster diameter.^[18,39,40] Thus, it seems that the subnanometer and nanometer classes of nanoclusters are the best candidates for displaying optical activity. This may be related to the fact that in this scale range, most of the metal atoms reside at the surface of the core and thus interact directly with the chiral ligands. Another explanation for the tendency of decreasing optical activity with increasing particle size is simply the increased configurational space for larger particles (larger number of gold atoms and ligands), and thus the increased probability of multiple energy minima on the potential-energy surface. An increasing number of conformers leads to decreased observable optical activity as positive and negative bands of different conformers average out. In contrast, optical activity was also reported by Park and co-workers for considerably larger Pen- or cysteine-capped silver particles (23.5 nm)^[76] and also for silver nanocrystals grown on a double-stranded DNA scaffold.^[77] However, these particles were not size-separated, and it can not be excluded that the observed optical activity is due to a fraction of small particles. Recently, this hypothesis was verified by Kimura and co-workers, who separated AgNPs according to their size and observed optical activity only for NPs in the nanometer range.^[40] Trends in the electronic transition frequencies and amplitudes with cluster size observed experimentally are qualitatively in agreement with both models.

4.2.3. Ligand Effect

When comparing the characteristics of all the ligands able to impart optical activity on the MBETs, it becomes evident that most of them, and especially cysteine derivatives, can undergo self-assembly mediated by hydrogen bonds. This property was proposed to be a crucial parameter for inducing optical activity.^[76,80] However, the atropisomeric bidentate ligands 1,1'-binaphthyl-2,2'-dithiol (BINAS) and 2,2'-bis-(diphenylphosphino)-1,1'-binaphthyl (BINAP) do not display such behavior, despite the fact that they are particularly well suited to impart optical activity.^[26,75] Indeed, BINAS-stabilized AuNPs have shown the largest optical activity reported so far for metal NPs, with a maximum anisotropy factor (g_{\max} factor) of 4×10^{-3} (see Table 1). On the other hand, a common feature is that all the ligands can interact with the cluster surface through at least two functional groups as also emphasized by the VCD studies on NIC. Furthermore, it was demonstrated that blocking the carboxyl group (anchoring point) in cysteine derivatives leads to loss of optical activity.^[76] Similarly, Kadodwala and co-workers have shown that (*R*)- and (*S*)-1-(1-naphthyl)ethylamine molecules adsorbed on a Cu(111) surface have three different chemical groups in close proximity to the surface and proved by optically active second-harmonic generation measurements that this multiple interaction imparts optical activity on the surface electronic structure, whereas 2-butanol with only one

interaction point does not.^[73] In contrast, Hegmann and co-workers studied the optical activity of small AuNPs covered by the chiral naproxen and observed that this molecule, which only has one interaction point and a long (C_{12}) spacer between the chiral center and the AuNPs surface, induces optical activity in MBETs.^[81] However, the observed optical activity was relatively weak. Rotello et al. have shown that chiral phenylalanine (Phe) more remote from the surface of the AuNPs (C_{24} spacer) does not induce optical activity in MBETs, despite the possibility of H-bonding and π - π interaction between the Phe moieties.^[82] These last two examples show that there is probably a relationship between the g_{\max} factor and the distance of the chiral center from the NP surface. This phenomenon suggests that mechanism B has an effect on the optical activity. However, we emphasize that these particles were not size-separated and that the weak optical activity can be related to the lack of small particles which have a larger CD signal or to the fact that the CD signals for different sizes of NPs cancel each other out.

5. Origin of Optical Activity in Metal-Based Electronic Transitions

5.1. X-Ray Diffraction Studies

Recently, the first total structure determination of a small gold-thiolate nanocluster composed of 102 gold atoms and 44 *p*-mercaptobenzoic acid (*p*-MBA) molecules was published.^[35] As shown in Figure 5, the particles are chiral and form a race-

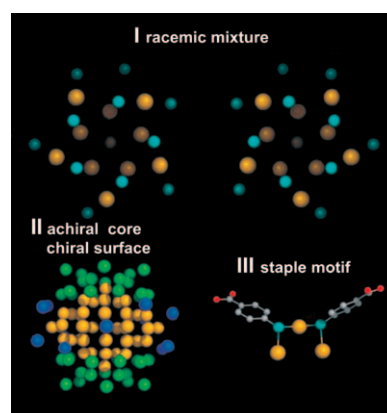


Figure 5. X-ray crystal structure determination of $Au_{102}(p\text{-MBA})_{44}$ NPs. I) View down the cluster axis of the two enantiomers (Au yellow, S cyan). II) Packing of gold atoms in the core. MD (2,1,2) in yellow, two 20-atom "caps" at the poles in green, and the 13-atom equatorial band in blue. III) Sulfur-gold interactions in the surface of the NPs. Example of two *p*-MBA molecules interacting with three gold atoms in a staple motif (Au yellow, S cyan, O red, C gray). Reprinted from Jadzinsky, Pablo D. et al., ref. [35], with permission from AAAS.

mic mixture in the crystal (I). However, the central gold atoms are packed in a Marks decahedron (MD) which is highly symmetric like the fcc structure of bulk gold (II). The chirality arises from the geometry of equatorial gold atoms on the surface. The deviations in local symmetry may reflect the interaction of the equatorial atoms with the adsorbed thiol. Furthermore,

most sulfur atoms bonded to two gold atoms in staple motifs are stereogenic centers (III). Therefore, even though the adsorbed thiol is achiral, the particles are chiral at two levels: I) the arrangement of the gold surface atoms and *p*-MBA molecules in the surface is chiral and II) most sulfur atoms are stereogenic centers.

Evidently, we can not assume that the structure of the central part of optically active AuNPs always resembles the achiral bulk metal structure. However, the crystal structure of the achiral thiolated AuNP [TOA]⁺[Au₂₅(SCH₂CH₂Ph)₁₈]⁻ (TOA⁺ = tetraoctylammonium) reported by Murray et al. reveals the same trend: a highly symmetric Au₁₃ core surrounded by six Au₂(SCH₂CH₂Ph)₃ staples.^[37] The latter structure has been surprisingly well predicted by DFT calculations.^[83] Based on the recently reported structures the arrangement of surface atoms (mechanism C) involved in the adsorption of thiols is now demonstrated to be a major element of chirality of thiolated AuNPs, whereas the intrinsic chirality of the core (mechanism A) has not been directly observed yet.

5.2. Post-Synthesis Ligand-Shell Perturbation and Modification

Several groups have monitored the evolution of optical activity in the MBETs of AuNPs on modification or perturbation of the organic layer. Yao and co-workers investigated the CD responses of D- and L-Pen-capped gold clusters as a function of temperature (20 and 40 °C) in water and the evolution of the chiroptical properties of the same NPs in toluene after a phase-transfer process.^[41] Two phenomena were pointed out. The first is an appreciable and reversible temperature dependence of the CD spectrum for the smallest (0.57 nm) NPs, whereas the CD spectra of the other NPs (1.18 and 1.75 nm) and the UV/Vis spectra of all the particles were almost invariant. The second is a perturbation of the CD spectra upon water/toluene phase transfer (measured only for the smallest NPs). The authors interpreted the results in terms of mechanism B (vicinal effect). Both temperature and phase transfer may act on the conformation of the adsorbed molecules, which shows that the latter plays a role in the optical activity of MBETs and the way in which chirality is transferred from the adsorbate to the metal particle.

The same group has also studied the chiral functionalization of optically inactive monolayer-protected silver nanoclusters by chiral ligand-exchange reactions.^[79] They found that the shape and the intensity of both optical and chiroptical responses in the MBETs depend on the enantiomeric excess (*ee*) of the chiral Pen on the silver cluster. The *g*_{max} factors are proportional to the *ee*. Furthermore, the measured anisotropy factors are considerably larger than those determined for Pen-stabilized gold particles. The authors speculated that a chiral deformation of the silver core (mechanism A) might be at the origin of this striking difference between the two metals.

At the same time, we have shown that the optical activity of Au₁₅ and Au₁₈ clusters protected with one enantiomer of NIC is reversed with a perfect mirror-image relationship on exchange for its opposite enantiomer under inert atmosphere (see

Figure 6).^[84] The cluster sizes were well retained during the "chiral inversion", as verified by gel electrophoresis and UV/Vis spectroscopy. The inversion of the optical activity in the MBETs

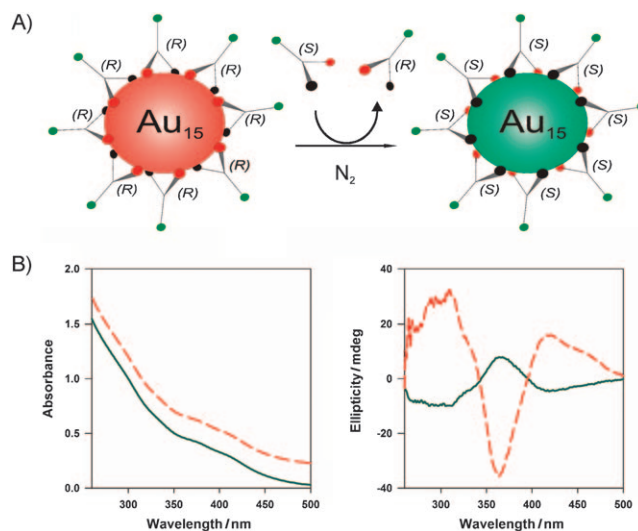


Figure 6. A) Schematic illustration of "chiral inversion" under inert atmosphere. The chiral adsorbed ligand is exchanged for its opposite enantiomer. B) UV/Vis (left) and CD spectra (right) of Au₁₅(NILC)₁₃ before (red dashed line) and after exchange with NIDC (green solid line). The spectra were recorded after size separation by PAGE. The UV/Vis spectra are normalized at 300 nm and offset for clarity. Reproduced with permission from ref. [84]. Copyright (2008) American Chemical Society.

was proportional to the *ee* of the ligand in the system. This experiment clearly demonstrates that the optical activity is dictated by the absolute configuration of the adsorbed thiols. It has been shown that the shape of the CD spectra originating from a chiral field (mechanism B) is strongly influenced by the number and arrangement of ligands.^[56] Over the course of the ligand-exchange reaction the chiral field is modified, but the spectral shapes are very similar, which seems to be an argument against chiral-field mechanism B and an indication for mechanism C. Whatever the nature of the chiral structure of the particles is (mechanisms A, B2, C), the optical isomerization implies that these structures are not stable enough in one enantiomeric form to withstand the driving force imposed by a switch of the absolute configuration of the adsorbed thiol.

6. Potential Applications

The interest in AuNPs is based on their potential applications in various fields such as biosensing,^[9] optics,^[85] electronics, photonics,^[13] catalysis,^[86] nanotechnology^[14] and drug or DNA delivery.^[11,87] Chiral AuNPs are particularly promising for asymmetry amplification at different length scales, that is, as chiral catalysts for chemical synthesis and chiral selective membranes or chiral dopants in liquid crystals (LCs). Further applications may be envisaged for the detection of chirality or may be related to the optical activity.

6.1. Chiral Catalysis

Metal NPs are potentially catalytically active and can also be used as catalyst supports. In the latter case the properties of homogeneous and heterogeneous catalysis are combined. For example, the catalytic properties of complexes supported on NPs can be influenced by the neighboring chiral ligands.^[88] Recently, an AuNP-supported multicomponent asymmetric catalyst was used in the Michael reaction of 2-cyclohexen-1-one with dibenzyl malonate affording the adduct in up to 67% yield and 98% *ee*.^[89] An advantage of such a catalyst is rapid separation from products and substrates by precipitation, membrane-based techniques, or SEC.

The intrinsic catalytic behavior of NPs has been widely examined. Many NPs proved to be efficient and selective catalysts not only for reactions that are also known to be catalyzed by molecular complexes, such as olefin hydrogenation or C-C coupling,^[90] but moreover for reactions which are not or are poorly catalyzed by molecular species, such as aromatic hydrogenation.^[91] Unambiguous distinction between colloidal and molecular catalysis is, however, often difficult.^[92–94] Chiral metal NPs can potentially combine the chirality of their core or surface and of their organic shell to induce enantioselectivity on prochiral substrates, as suggested previously for organometallic clusters with a chiral framework.^[58–68] Despite the impressive progress in catalysis, however, only a few NP systems were found to be efficient in asymmetric catalysis till today.^[75,86,95–103] The most relevant systems involve Pt and Pd NPs stabilized by cinchonidine, in the hydrogenation of pyruvate derivatives with *ee* up to 95–98%.^[95,97–100,104,105]

Gold catalysis has become a hot topic and many published examples have demonstrated benefits of gold catalysts such as higher activity, milder conditions, and higher selectivity and enantioselectivity.^[106–109] However, so far there is only one promising example of a preliminary test of enantioselective catalysis using chirally modified AuNPs with Pd-mediated reactivity.^[110] This is probably due to the fact that gold catalysis is relatively new and that chiral AuNPs are even more recent.

6.2. Nanoparticles in Liquid-Crystal Media

Control of the organization of NPs in order to integrate them into high-tech devices such as waveguides, band-gap materials, light-scattering devices, flat panels, and perfect lenses while avoiding use of the top-down approach remains a challenge in nanotechnology. Liquid-crystalline materials appear to be perfect candidates for controlling the crucial parameters of size, shape, and self-assembly of nanoscale materials in a one-pot process. The use of LCs in syntheses and self-assembly was recently reviewed by Hegmann and co-workers.^[111] Organization of nanomaterials in LCs can furthermore respond to external stimuli such as an electric (magnetic) field or temperature. This opens the possibility to use such composites as electrical actuators.

Figure 7 shows that achiral NPs coated with a zwitterionic surfactant when dispersed in a cholesteric LC can order in accordance with the chiral helical structure of the chiral phase.

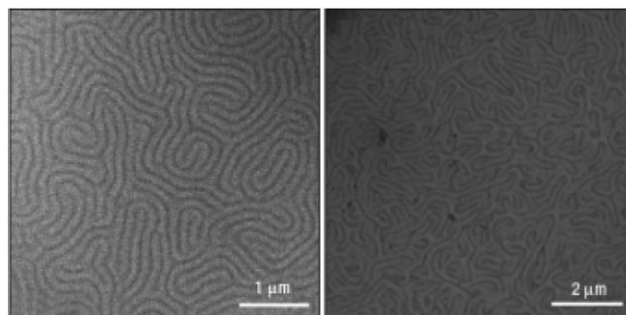


Figure 7. TEM images of the fingerprint cholesteric texture for the chiral liquid-crystalline material in pure form (left) and doped with achiral NPs (right). Reprinted with permission from Macmillan Publishers Ltd: Nature Materials, ref. [112], copyright (2002).

The platinum NPs form periodic ribbons, which mimic the well-known cholesteric texture. De Guerville et al. also demonstrated that the NPs not only decorate the pristine structure but create a novel structure characterized by a larger periodicity.^[112,113] They also observed that this periodicity, that is, the distance between the ribbons, can be tuned by varying the molar fraction of chiral mesogens present in the pure cholesteric host. On the contrary, Hegmann and Qi demonstrated that C₁₂Napr*-capped AuNPs (C₁₂Napr* = naproxen-functionalized dodecanethiolate) can be used to induce chirality on a nonchiral nematic LC phase.^[81] The use of AuNPs protected with chiral ligand as chiral dopant in an LC phase was furthermore confirmed by induced CD studies on a nematic LC (NLC) doped with three different NPs. This experiment revealed transfer of chirality from the NPs to the NLC phase to form a chiral nematic phase with opposite helical sense in comparison to the pure chiral ligand dispersed in the same NLC host.^[114] The formed stripe texture may be tunable according to the size of the NPs or their functionality. Nematic LCs doped with gold nanoclusters can be aligned and electrically reoriented at lower threshold voltages than pure NLCs.^[115] This opens a pathway for improving LC mixtures for a variety of applications such as liquid-crystal displays.

6.3. Optics

Rosi and co-workers recently published a new bottom-up peptide-based method for the design and synthesis of highly ordered AuNP double helices (see Figure 8).^[115] Such stereochemical arrangement of NPs is expected to be of great importance for potential applications derived from their plasmonic properties. In the visible to near-IR part of the spectrum, the normal incidence transmission of circularly polarized light through the metallic nanostructured anisotropic planar chiral metamaterial is asymmetric in the opposite direction.^[116] This phenomenon can be used in the field of polarization-sensitive devices. A quantum chemical approach to the design of chiral negative-index materials has shown that this can be achieved by introducing sharp plasmonic resonances with metal NPs.^[117]

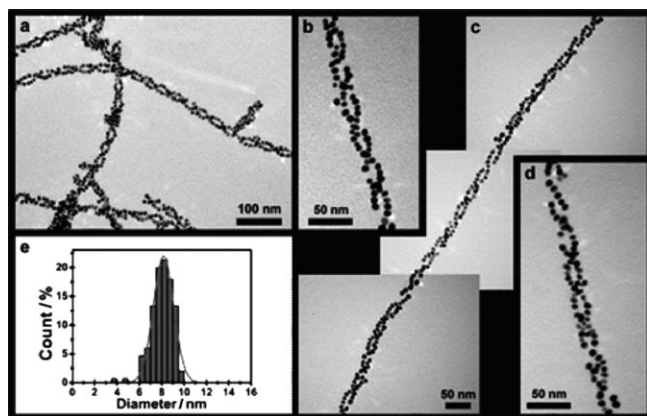


Figure 8. a)–d) TEM characterization of AuNP double helices. e) The size of the AuNPs is uniform (8.2 ± 1.0 nm, based on 150 counts). Reproduced with permission from ref. [15]. Copyright (2006) American Chemical Society.

6.4. Chiral Discrimination

Self-assembled monolayers of chiral thiols on metal surfaces have proved their potential for enantiodiscrimination.^[50] On account of their high specific surface area, chiral NPs should be even more interesting for discrimination. Kong and co-workers have already shown that AuNPs are efficient sensors capable of probing chiral amino acids at the subpicomolar level. The signal was monitored by differential potential voltammetry with a glassy carbon electrode modified with bovine serum albumin, which is a chiral modifier, and amplified by silver atoms anchored on the AuNPs.^[118] Similarly, Rotello et al. have clearly demonstrated by calorimetric studies that NPs bearing enantiomeric and diastereoisomeric end groups have distinctly different binding affinities towards protein targets.^[82] They further demonstrated that trimethylammonium-functionalized AuNPs protected with mixed monolayers can stabilize peptides in water through favorable interactions on templation of the NPs to the peptide surface.^[119] This enhances the potential of AuNPs in helix recognition. Recently, colloidal AgNPs coated with GSH were used as electromagnetic antennae.^[120] It was shown that the absorption and CD spectra of bimane, a chromophore, were enhanced when attached to NPs. The chromophore absorbs at the surface-plasmon-resonance wavelength of the AgNPs. The enhancement by two orders of magnitude of the induced CD bands of GSH–bimane with the AgNPs is similar to the other surface-enhanced optical phenomena.^[121–123] This strategy should enable the observation of weak induced CD of chromophores by enhancing them to typical values of UV and CD of amino and nucleic acids. This reveals that chirality on NPs is an important prerequisite for the specific recognition required for therapeutic applications.

7. Outlook

Nanoscience is still in the discovery phase, and this is particularly true for chiral NPs. Only very few examples of well-defined optically active NPs have been synthesized and only on a small scale (milligrams). However, examples of applications described

in the last section show the great potential of chiral NPs, for example, in enantioselective catalysis, LC displays, and chiral recognition. Progress in enantioselective synthesis and resolution of chiral NPs is expected in the near future. Integration of NPs into larger systems may allow preparation of nanoscale optical components^[25] and planar polarization-sensitive devices.^[23] The merging of optical activity with surface plasmons may pave the way for new types of “chiroptonic devices”. Nanoparticles are already starting materials or catalysts for the preparation of larger anisotropic nanomaterials such as nanorods. Perhaps chiral NPs will allow the preparation of larger chiral nanomaterials. Finally, chiral NPs are also of fundamental interest as nanosize analogues of extended chiral metal surfaces and serve as models for better understanding of interactions between surfaces and organic molecules.

Acknowledgements

Financial support by the Swiss National Science Foundation is kindly acknowledged.

Keywords: chirality · circular dichroism · gold · nanostructures · organic–inorganic hybrid composites

- [1] S. Chen, R. S. Ingram, M. J. Hostetler, J. J. Pietron, R. W. Murray, T. G. Schaaff, J. T. Khoury, M. M. Alvarez, R. L. Whetten, *Science* **1998**, *280*, 2098.
- [2] C. L. Cleveland, U. Landman, T. G. Schaaff, M. N. Shafiqullin, P. W. Stephens, R. L. Whetten, *Phys. Rev. Lett.* **1997**, *79*, 1873.
- [3] G. Wang, T. Huang, R. W. Murray, L. Menard, R. G. Nuzzo, *J. Am. Chem. Soc.* **2005**, *127*, 812.
- [4] Y. Yang, S. Chen, *Nano Lett.* **2003**, *3*, 75.
- [5] J. P. Wilcoxon, P. Provencio, *J. Phys. Chem. B* **2003**, *107*, 12949.
- [6] K. Nunokawa, S. Onaka, M. Ito, M. Horibe, T. Yonezawa, H. Nishihara, T. Ozeki, H. Chiba, S. Watase, M. Nakamoto, *J. Organomet. Chem.* **2006**, *691*, 638.
- [7] J. Ramírez, M. Sanaú, E. Fernández, *Angew. Chem.* **2008**, *120*, 5272; *Angew. Chem. Int. Ed.* **2008**, *47*, 5194.
- [8] I. Dolamic, C. Gautier, J. Boudon, N. Shalkevich, T. Bürgi, *J. Phys. Chem. C* **2008**, *112*, 5816.
- [9] N. L. Rosi, C. A. Mirkin, *Chem. Rev.* **2005**, *105*, 1547.
- [10] H. Wohltjen, A. W. Snow, *Anal. Chem.* **1998**, *70*, 2856.
- [11] R. Hong, G. Han, J. M. Fernandez, B. j. Kim, N. S. Forbes, V. M. Rotello, *J. Am. Chem. Soc.* **2006**, *128*, 1078.
- [12] H. Fan, K. Yang, D. M. Boye, T. Sigmon, K. J. Malloy, H. Xu, G. P. Lopez, C. J. Brinker, *Science* **2004**, *304*, 567.
- [13] W. L. Barnes, A. Dereux, T. W. Ebbesen, *Nature* **2003**, *424*, 824.
- [14] M. C. Daniel, D. Astruc, *Chem. Rev.* **2004**, *104*, 293.
- [15] C.-L. Chen, P. Zhang, N. L. Rosi, *J. Am. Chem. Soc.* **2008**, *130*, 13555.
- [16] S. A. Maier, H. A. Atwater, *J. Appl. Phys.* **2005**, *98*, 011101.
- [17] Z. Tang, N. A. Kotov, *Adv. Mater.* **2005**, *17*, 951.
- [18] C. Gautier, T. Bürgi, *J. Am. Chem. Soc.* **2006**, *128*, 11079.
- [19] C. F. McFadden, P. S. Cremer, A. J. Gellman, *Langmuir* **1996**, *12*, 2483.
- [20] S. M. Barlow, R. Raval, *Curr. Opin. Colloid Interface Sci.* **2008**, *13*, 65.
- [21] L. A. Nafie, *Annu. Rev. Phys. Chem.* **1997**, *48*, 357.
- [22] T. B. Freedman, X. Cao, R. K. Dukor, L. A. Nafie, *Chirality* **2003**, *15*, 743.
- [23] V. Tuomas, J. Konstantins, T. Jari, V. Pasi, S. Yuri, *Appl. Phys. Lett.* **2003**, *83*, 234.
- [24] S. Yuri, Z. Nikolay, O. Michail, *Appl. Phys. Lett.* **2001**, *78*, 498.
- [25] B. Canfield, S. Kujala, K. Laiho, K. Jefimovs, J. Turunen, M. Kauranen, *Plasmonics: Metallic Nanostructures and their Optical Properties III*, Vol. 5927 (Ed.: I. S. Mark), SPIE, **2005**, p. 59270C.
- [26] Y. Yanagimoto, Y. Negishi, H. Fujihara, T. Tsukuda, *J. Phys. Chem. B* **2006**, *110*, 11611.

- [27] M. Brust, M. Walker, D. Bethell, D. J. Schiffrin, R. Whyman, *J. Chem. Soc. Chem. Commun.* **1994**, 801.
- [28] G. H. Woehle, J. E. Hutchison, *Inorg. Chem.* **2005**, *44*, 6149.
- [29] J. Turkevich, P. Stevenson, J. Hillier, *Discuss. Faraday Soc.* **1951**, *11*, 55.
- [30] G. Schmid, *Inorg. Synth.* **1990**, *27*, 214.
- [31] Y. Song, T. Huang, R. W. Murray, *J. Am. Chem. Soc.* **2003**, *125*, 11694.
- [32] Y. Shichibu, Y. Negishi, T. Tsukuda, T. Teranishi, *J. Am. Chem. Soc.* **2005**, *127*, 13464.
- [33] R. Balasubramanian, R. Guo, A. J. Mills, R. W. Murray, *J. Am. Chem. Soc.* **2005**, *127*, 8126.
- [34] Y. Shichibu, Y. Negishi, H. Tsunoyama, M. Kanehara, T. Teranishi, T. Tsukuda, *Small* **2007**, *3*, 835.
- [35] P. D. Jadzinsky, G. Calero, C. J. Ackerson, D. A. Bushnell, R. D. Kornberg, *Science* **2007**, *318*, 430.
- [36] M. Zhu, C. M. Aikens, F. J. Hollander, G. C. Schatz, R. Jin, *J. Am. Chem. Soc.* **2008**, *130*, 5883.
- [37] M. W. Heaven, A. Dass, P. S. White, K. M. Holt, R. W. Murray, *J. Am. Chem. Soc.* **2008**, *130*, 3754.
- [38] T. G. Schaaff, G. Knight, M. N. Shafiqullin, R. F. Borkman, R. L. Whetten, *J. Phys. Chem. B* **1998**, *102*, 10643.
- [39] H. Yao, K. Miki, N. Nishida, A. Sasaki, K. Kimura, *J. Am. Chem. Soc.* **2005**, *127*, 15536.
- [40] N. Nishida, H. Yao, T. Ueda, A. Sasaki, K. Kimura, *Chem. Mater.* **2007**, *19*, 2831.
- [41] H. Yao, T. Fukui, K. Kimura, *J. Phys. Chem. C* **2007**, *111*, 14968.
- [42] C. Gautier, R. Taras, S. Gladioli, T. Bürgi, *Chirality* **2008**, *20*, 486.
- [43] L. A. Nafie, T. A. Keiderling, P. J. Stephens, *J. Am. Chem. Soc.* **1976**, *98*, 2715.
- [44] C. N. Su, T. A. Keiderling, *J. Am. Chem. Soc.* **1980**, *102*, 511.
- [45] R. Schweitzer-Stenner, F. Eker, K. Griebenow, X. Cao, L. A. Nafie, *J. Am. Chem. Soc.* **2004**, *126*, 2768.
- [46] P. Bour, H. Navratilova, V. Setnicka, M. Urbanova, K. Volka, *J. Org. Chem.* **2002**, *67*, 161.
- [47] T. Bürgi, A. Vargas, A. Baiker, *J. Chem. Soc. Perkin Trans. 2* **2002**, 1596.
- [48] C. Gautier, T. Bürgi, *Chem. Commun.* **2005**, 5393.
- [49] C. Gautier, M. Bieri, I. Dolamic, S. Angeloni, J. Boudon, T. Bürgi, *Chimia* **2006**, *60*, 777.
- [50] M. Bieri, C. Gautier, T. Bürgi, *Phys. Chem. Chem. Phys.* **2007**, *9*, 671.
- [51] C. Gautier, T. Bürgi, *Chimia* **2008**, *62*, 465.
- [52] C. Gautier, T. Bürgi in *Chirality at the Nanoscale: Nanoparticles, Surfaces, Materials and More, Vol. 1* (Ed.: D. B. Amabilino), Wiley-VCH, Weinheim, **2009**, p. 380.
- [53] T. L. Wetzell, A. E. DePristo, *J. Chem. Phys.* **1996**, *105*, 572.
- [54] E. K. Parks, K. P. Kerns, S. J. Riley, *J. Chem. Phys.* **1998**, *109*, 10207.
- [55] I. L. Garzón, M. R. Beltrán, G. Gonzalez, I. Gutierrez-Gonzalez, K. Michaelian, J. A. Reyes-Nava, J. I. Rodríguez-Hernandez, *Eur. Phys. J. D* **2003**, *24*, 105.
- [56] M. R. Goldsmith, C. B. George, G. Zuber, R. Naaman, D. H. Waldeck, P. Wipf, D. N. Beratan, *Phys. Chem. Chem. Phys.* **2006**, *8*, 63.
- [57] V. Humblot, S. Haq, C. Muryn, W. A. Hofer, R. Raval, *J. Am. Chem. Soc.* **2002**, *124*, 503.
- [58] H. Beurich, H. Vahrenkamp, *Angew. Chem.* **1978**, *90*, 915; *Angew. Chem. Int. Ed. Engl.* **1978**, *17*, 863.
- [59] M. Müller, H. Vahrenkamp, *Chem. Ber.* **1983**, *116*, 2748.
- [60] P. Gusbeth, H. Vahrenkamp, *Chem. Ber.* **1985**, *118*, 1746.
- [61] D. Mani, H. Vahrenkamp, *Chem. Ber.* **1986**, *119*, 3639.
- [62] P. Bladon, P. L. Pauson, H. Brunner, R. Eder, *J. Organomet. Chem.* **1988**, *355*, 449.
- [63] R. D. Adams, *Catalysis by Di- and Polynuclear Metal Cluster Complexes*, Wiley, New York, **1998**.
- [64] K. Oyaizu, E. Tsuchida, *J. Am. Chem. Soc.* **1998**, *120*, 237.
- [65] S. P. Tunik, T. S. Pilyugina, I. O. Koshevoy, S. I. Selivanov, M. Haukka, T. A. Pakkanen, *Organometallics* **2004**, *23*, 568.
- [66] L. Vieille-Petit, G. Suss-Fink, B. Therrien, T. R. Ward, H. Stoeckli-Evans, G. Labat, L. Karmazin-Brelot, A. Neels, T. Bürgi, R. G. Finke, C. M. Hagen, *Organometallics* **2005**, *24*, 6104.
- [67] M. Feliz, E. Guillaumon, R. Llusar, C. Vicent, S. E. Stiriba, J. Pérez-Prieto, M. Barberis, *Chem. Eur. J.* **2006**, *12*, 1486.
- [68] V. D. Reddy, *J. Organomet. Chem.* **2006**, *691*, 27.
- [69] I. L. Garzón, J. A. Reyes-Nava, J. I. Rodríguez-Hernández, I. Sigal, M. R. Beltrán, K. Michaelian, *Phys. Rev. B* **2002**, *66*, 073403.
- [70] M. Bieri, T. Bürgi, *J. Phys. Chem. B* **2005**, *109*, 22476.
- [71] M. Bieri, T. Bürgi, *Langmuir* **2005**, *21*, 1354.
- [72] M. Bieri, T. Bürgi, *Phys. Chem. Chem. Phys.* **2006**, *8*, 513.
- [73] A. Mulligan, I. Lane, G. B. D. Rousseau, S. M. Johnston, D. Lennon, M. Kadodwala, *Angew. Chem.* **2005**, *117*, 1864.
- [74] H. Häkkinen, M. Walter, H. Gronbeck, *J. Phys. Chem. B* **2006**, *110*, 9927.
- [75] M. Tamura, H. Fujihara, *J. Am. Chem. Soc.* **2003**, *125*, 15742.
- [76] T. Li, H. G. Park, H. S. Lee, S. H. Choi, *Nanotechnology* **2004**, *15*, S660.
- [77] G. Shemer, O. Krichevski, G. Markovich, T. Molotsky, I. Lubitz, A. B. Kotlyar, *J. Am. Chem. Soc.* **2006**, *128*, 11006.
- [78] M. P. Moloney, Y. K. Gun'ko, J. M. Kelly, *Chem. Commun.* **2007**, 3900.
- [79] N. Nishida, H. Yao, K. Kimura, *Langmuir* **2008**, *24*, 2759.
- [80] N. Bovet, N. McMillan, N. Gadegaard, M. Kadodwala, *J. Phys. Chem. B* **2007**.
- [81] H. Qi, T. Hegmann, *J. Mater. Chem.* **2006**, *16*, 4197.
- [82] C.-C. You, S. S. Agasti, V. M. Rotello, *Chem. Eur. J.* **2008**, *14*, 143.
- [83] J. Akola, M. Walter, R. L. Whetten, H. Häkkinen, H. Gronbeck, *J. Am. Chem. Soc.* **2008**, *130*, 3756.
- [84] C. Gautier, T. Bürgi, *J. Am. Chem. Soc.* **2008**, *130*, 7077.
- [85] S. Sun, C. B. Murray, D. Weller, L. Folks, A. Moser, *Science* **2000**, *287*, 1989.
- [86] S. Jansat, M. Gomez, K. Philippot, G. Muller, E. Guieu, C. Claver, S. Castillon, B. Chaudret, *J. Am. Chem. Soc.* **2004**, *126*, 1592.
- [87] S. Kommareddy, M. Amiji, *Nanomedicine: NBM* **2007**, *3*, 32.
- [88] T. Belser, M. Stohr, A. Pfaltz, *J. Am. Chem. Soc.* **2005**, *127*, 8720.
- [89] S. Takizawa, M. L. Patil, K. Marubayashi, H. Sasai, *Tetrahedron* **2007**, *63*, 6512.
- [90] A. Roucoux, J. Schulz, H. Patin, *Chem. Rev.* **2002**, *102*, 3757.
- [91] J. A. Widegren, R. G. Finke, *J. Mol. Catal. A* **2003**, *191*, 187.
- [92] I. W. Davies, L. Matty, D. L. Hughes, P. J. Reider, *J. Am. Chem. Soc.* **2001**, *123*, 10139.
- [93] J. A. Widegren, R. G. Finke, *J. Mol. Catal. A* **2003**, *198*, 317.
- [94] A. K. Diallo, C. Ornelas, L. Salmon, J. Ruiz Aranzaes, D. Astruc, *Angew. Chem.* **2007**, *119*, 8798; *Angew. Chem. Int. Ed.* **2007**, *46*, 8644.
- [95] H. Bönemann, G. A. Braun, *Angew. Chem.* **1996**, *108*, 2120; *Angew. Chem. Int. Ed. Engl.* **1996**, *35*, 1992.
- [96] M. Studer, H. U. Blaser, C. Exner, *Adv. Synth. Catal.* **2003**, *345*, 45.
- [97] H. Bönemann, G. A. Braun, *Chem. Eur. J.* **1997**, *3*, 1200.
- [98] X. Zuo, H. Liu, D. Guo, X. Yang, *Tetrahedron* **1999**, *55*, 7787.
- [99] J. U. Köhler, J. S. Bradley, *Catal. Lett.* **1997**, *45*, 203.
- [100] J. U. Köhler, J. S. Bradley, *Langmuir* **1998**, *14*, 2730.
- [101] V. Mevellec, C. Mattioda, J. Schulz, J. P. Rolland, A. Roucoux, *J. Catal.* **2004**, *225*, 1.
- [102] S. Jansat, D. Picurelli, K. Pelzer, K. Philippot, M. Gomez, G. Muller, P. Le-cante, B. Chaudret, *New J. Chem.* **2006**, *30*, 115.
- [103] K. Nasar, F. Fache, M. Lemaire, J. C. Beziat, M. Besson, P. Gallezot, *J. Mol. Catal.* **1994**, *87*, 107.
- [104] Y. Orito, S. Imai, S. Nawa, I. Nguyeng, *J. Synth. Org. Chem. Jpn.* **1979**, *37*, 173.
- [105] T. Bürgi, A. Baiker, *Acc. Chem. Res.* **2004**, *37*, 909.
- [106] G. C. Bond, *Catal. Today* **2002**, *72*, 5.
- [107] A. S. K. Hashmi, *Angew. Chem.* **2005**, *117*, 7150; *Angew. Chem. Int. Ed.* **2005**, *44*, 6990.
- [108] G. Bond, *Gold Bull.* **2004**, *41* 235.
- [109] A. W. Ross, *Chem. Eur. J.* **2008**, *14*, 5382.
- [110] M. J. Oila, A. M. P. Koskinen, *ARKIVOC* **2006**, *15*, 76.
- [111] T. Hegmann, H. Qi, V. M. Marx, *J. Inorg. Organomet. Polym. Mater.* **2006**, *483*.
- [112] M. Mitov, C. Portet, C. Bourgerette, E. Snoeck, M. Verelst, *Nat. Mater.* **2002**, *1*, 229.
- [113] M. Mitov, C. Bourgerette, F. de Guerville, *J. Phys. Condens. Matter* **2004**, *16*, S1981.
- [114] H. Qi, J. O'Neil, T. Hegmann, *J. Mater. Chem.* **2008**, *18*, 374.
- [115] H. Qi, B. Kinkead, T. Hegmann, *Adv. Funct. Mater.* **2008**, *18*, 212.
- [116] V. A. Fedotov, A. S. Schwanecke, N. I. Zheludev, V. V. Khardikov, S. L. Prosvirnin, *Nano Lett.* **2007**, *7*, 1996.
- [117] A. Baev, M. Samoc, P. N. Prasad, M. Krykunov, J. Autschbach, *Opt. Express* **2007**, *15*, 5730.
- [118] Y. Wang, X. Yin, M. Shi, W. Li, L. Zhang, J. Kong, *Talanta* **2006**, *69*, 1240.
- [119] A. Verma, H. Nakade, J. M. Simard, V. M. Rotello, *J. Am. Chem. Soc.* **2004**, *126*, 10806.

- [120] I. Lieberman, G. Shemer, T. Fried, E. M. Kosower, G. Markovich, *Angew. Chem.* **2008**, *120*, 4933.
- [121] M. Moskovits, *J. Chem. Phys.* **1978**, *69*, 4159.
- [122] K. Kneipp, H. Kneipp, I. Itzkan, R. R. Dasari, M. S. Feld, *Chem. Rev.* **1999**, *99*, 2957.

- [123] C. L. Haynes, R. P. Van Duyne, *J. Phys. Chem. B* **2003**, *107*, 7426.

Received: October 28, 2008

Published online on January 13, 2009
